Published in final edited form as:
J Biomed Mater Res B Appl Biomater. 2011 July ; 98(1): 160–170. doi:10.1002/jbm.b.31831.

Direct-write Bioprinting Three-Dimensional Biohybrid Systems for Future Regenerative Therapies

Carlos C. Chang, **Eugene D. Boland**, **Stuart K. Williams**, and **James B. Hoying**
Cardiovascular Innovation Institute, 302 E Muhammad Ali Blvd, Louisville, KY 40202

Abstract

Regenerative medicine seeks to repair or replace dysfunctional tissues with engineered biological or biohybrid systems. Current clinical regenerative models utilize simple uniform tissue constructs formed with cells cultured onto biocompatible scaffolds. Future regenerative therapies will require the fabrication of complex three-dimensional constructs containing multiple cell types and extracellular matrices. We believe bioprinting technologies will provide a key role in the design and construction of future engineered tissues for cell-based and regenerative therapies. This review describes the current state-of-the-art bioprinting technologies, focusing on direct-write bioprinting. We describe a number of process and device considerations for successful bioprinting of composite biohybrid constructs. In addition, we have provided baseline direct-write printing parameters for a hydrogel system (Pluronic F127) often used in cardiovascular applications. Direct-write dispensed lines (gels with viscosities ranging from 30 mPa*s to greater than 600×10^6 mPa*s) were measured following mechanical and pneumatic printing via three commercially available needle sizes (20ga, 25ga, and 30ga). Example patterns containing microvascular cells and isolated microvessel fragments were also bioprinted into composite 3D structures. Cells and vessel fragments remained viable and maintained in vitro behavior after incorporation into biohybrid structures. Direct-write bioprinting of biologicals provides a unique method to design and fabricate complex, multi-component 3D structures for experimental use. We hope our design insights and baseline parameter descriptions of direct-write bioprinting will provide a useful foundation for colleagues to incorporate this 3D fabrication method into future regenerative therapies.

Keywords

Bioprinting; Regenerative Medicine; Tissue Engineering; Hydrogels; Biohybrid Devices

Introduction

Regenerative medicine aims to develop new methods to treat and restore function to damaged and dysfunctional tissue, achieving these therapies with systems that not only contain [1], but are designed in concert with biologicals. From simple scaffolds [2], to bioactive materials [3], therapeutic agents are often applied directly to target tissues, particularly for cardiovascular therapies [4]. Depending on the extent of tissue damage and dysfunction, simple augmentation or repair may not be sufficient. For these cases, investigators have begun developing engineered tissues. Scientists have already fabricated and clinically used artificial trachea [5], bladders [6], and skin [7]. These examples rely on thin, degradable scaffolds that are populated with harvested autologous cells from the patient. After a period of *in vitro* culture, the tissue constructs were surgically grafted back into the patient. Although

Corresponding Author: James B. Hoying, jay.hoying@louisville.edu, 502.852.1381 (p), 502.852.1795 (f).

favorable results have been realized, these artificial “tissues” are structurally simple; one or two cell types are grown on the scaffold yielding a therapeutic tissue with uniform properties. These engineered tissues lack many of the characteristics found in typical biological tissues, such as complex organization of multiple cell types, complex extracellular matrices, and an invested microvasculature.

As the development of regenerative therapies progresses, investigators will need tools that allow the design and fabrication of more complex tissues. Researchers will need the capability to form three-dimensional (3D) tissue volumes that contain a variety of extracellular matrices (ECM), cells, and combinations thereof; systems that permit complex organization of these biological materials into homogeneous or heterogeneous layers. Investigators will need systems that facilitate the incorporation of a microvasculature within these engineered tissues. We believe biological printing, or bioprinting, will be a key technology that will enable future fabrication of complex biohybrid systems. *The following discussion describes current state-of-the-art bioprinting technologies used to fabricate three-dimensional biological structures and includes the focus of this review, layer-by-layer fabrication via direct-write bioprinting*[8]. We hope the fundamental instrument, environment, and fabrication parameters provided in this manuscript will assist the adoption of bioprinting technologies for future development of regenerative technologies.

Three-dimensional Tissue Fabrication

In recent years, there have been many advances in three-dimensional (3D) fabrication of biological structures. In particular, investigators are beginning to develop methods that permit the design and fabrication of 3D volumes composed of biological materials and viable cells. Three prominent fabrication methods include soft lithography [9–14], rapid prototyping [15–19], and bioprinting [8,20]. All three permit the organization of proteins and ECM that successfully direct cell growth in designed two-dimensional (2D) and 3D patterns. However, constructs engineered by each technique vary greatly in terms of fabrication method and means of cell incorporation.

Soft Lithography is a micro-electro mechanical systems (MEMS) derivative technology, requiring the fabrication of a master pattern that is used to form subsequent molds. Depending on the desired mold resolution, initial patterns may be fabricated with traditional MEMS techniques (such as silicon wafer or glass etching, photoresist film processing), photo- or transparency masks, or micromachined parts[21]. The polymer typically used to form molds for experimental use is poly(dimethyl) siloxane (PDMS). By using an elastomer such as PDMS, SL molds may have fine feature resolution, compatibility with biological functionality (surfaces may be chemically altered with biological proteins)[12], and permit the serial or simultaneous formation of small 3D volumes of cells and ECM [9]. However, once a pattern and derived molds are fabricated, they cannot be easily changed. If a design modification is desired, a new pattern must be designed and fabricated, followed by the generation of new molds. Depending on the pattern, these steps may be a time consuming and expensive process. Also, SL patterns are typically precise protrusions, channels, or raised shapes from a flat surface. If a multi-layer construct is desired, multiple masks and patterns may be required [22]. Moreover, multiple molds may require specialized equipment to precisely align each layer [23]. Photomasks [24], microchannels [25], and SL molds [26] have also been used to form small modular hydrogel volumes. These microgels then self-assemble into 3D structures based on surface chemistries and concentration. However, it may be challenging to control precise 3D organization and interior features of such components.

Unlike the inherently planar structures associated with SL fabrication and low resolution assembly of microgels, a number of rapid prototyping (RP) techniques were designed to

precisely fabricate complex freestanding 3D structures [27]. RP designs begin with a computer generated volumetric form. This form is commonly translated into an actual 3D structure by breaking the volume down into a series of layers. These layers are then constructed by the RP device. There are a wide range of RP technologies that have been utilized to fabricate "biological" structures. For instance, laser-sintering has been used to form 3D bone-like hydroxyapatite scaffolds [17]. Likewise, extrusion freeforming has been utilized to control the size and porosity of green hydroxyapatite scaffolds prior to traditional sintering [28]. Stereolithography and multiphoton lithography advancements have led to polymerization of complex microscale 3D structures [29], including biological scaffolds [18] with precise control of internal microstructure and porosity [19]. However, typically used materials, solvents, and device components in RP techniques, such as laser-sintering, extrusion freeforming, and stereolithography, are not amenable to cellular incorporation as the structure is fabricated [27]. Such 3D scaffolds are typically fabricated first and then treated and inoculated with additional biological or cellular components. As research moves forward, 3D fabrication techniques will be required to incorporate biological and cellular components as the structure is being constructed, not as a secondary step [30]. This work has begun in a specialized type of rapid prototyping, bioprinting.

Bioprinting fabrication is focused on the precise deposition of biological materials (such as ECM proteins, cells, and cell-matrix suspensions) into 3D structures. Currently, there are two prominent methods of bioprinting, ink-jet-based bioprinting [20] and direct-write bioprinting [8]. A comparison of printing features is outlined in Table 1. Ink-jet bioprinting was first introduced as a method to construct biological structures from the "bottom up" (layer-by-layer fabrication starting with the bottom most layer of a structure and depositing successive layers onto previously deposited layers). Ink-jet bioprinters eject fluid droplets onto a surface to reproduce a rasterized (or point-by-point) translation of a designed pattern (Figure 1). In order to print biologicals, researchers modify commercial print heads to accommodate commercial needles [20,31] or custom needles and nozzles [32–35]. Researchers then replace commercial printing ink with "bio-ink", such as proteins [35], enzymes [36], and cells suspended in media or saline [31]. In recent years, investigators have expanded to print from thin hydrogel films using modified thermal [36] and laser printer systems [33]. In contrast, direct-write bioprinting utilizes computer-controlled actuators to dispense dots or lines of material onto a surface via mechanical and/or pneumatic power [8] (Figure 1). In common configurations [8,37,38], these systems extrude bio-inks utilizing standard syringes and needles. Computer controlled stage movements in x, y, and z directions permit layer-by-layer deposition of materials.

Bioprinting a structure is a complicated, multivariable process and is affected by properties of both material and printing device. The size of the printed material is determined by the interaction of a number of factors, including dispensing orifice dimension, solvent, fluid viscosity, surface tension, fluid-surface interactions, polymer concentration, humidity, and temperature [33,35,36]. To complicate the printing process, many of these variables are influenced by each other. For instance, a temperature sensitive hydrogel, such as collagen, will begin to polymerize and irreversibly increase viscosity as temperature increases. This increased viscosity will require parameter modifications in order to maintain adequate material dispensing.

All direct-write bioprinting systems, both custom and commercial, are designed to dispense a material onto a surface. Typically, materials are dispensed from a syringe [8,39,40] or reservoir [37,41]. A few systems permit precise serial dispensing of multiple materials without retooling [8,32]; multiple printing units are built into the bioprinter hardware and software. Each printing unit is controlled independently and may be loaded with similar or dissimilar materials. In this manner, unique combinations of materials and compositions may be used.

Fortunately, bioprinted patterns are easily designed, modified, printed, and changed on the fly. For example, *our BioArchitecture Tool (BAT) system permits pattern generation* by either importing a Computer-Aided Design (CAD) drawing, tracing a vector pattern from an image, or directly coding 3D coordinates into the system [8]. CAD files are easily updated and coding can be readily manipulated at any time. In this manner, a bioprinted pattern may be changed in seconds to minutes instead of days to weeks (a typical turn-around time for SL-based mold fabrication). Moreover, *quick turn-around time lends bioprinting to custom fabrication of structures for individual* applications, such as matching the shape of a wound geometry or forming tissue-specific replacements grafts post-biopsy or post-surgery.

Material Selection

A major difference between ink-jet and direct-write bioprinting systems is the range of compatible materials and viscosities. Table 1 describes key differences between these two printing technologies. Typically, ink-jet printed biological materials are low viscosity suspensions or hydrogels that may or may not contain suspended cells [8,37–40]. Likewise, initial research efforts in direct-write bioprinting focused on deposition of low viscosity hydrogels into simple patterns onto biocompatible surfaces [8,40]. Due to printing limitations of these materials (discussed in greater detail in *Direct-write Printing Parameters*), more complex 3D structures were difficult to realize. As a result, our laboratory has moved on to direct-write bioprint composite structures that include serial printing of two materials – biocompatible structural elements and biological materials. In our “mold and fill” printing strategy, a high viscosity hydrogel is dispensed to form a mold that defines the shape of subsequently printed low-viscosity biological materials (Figure 2).

A major challenge of bioprinting, before developing patterns and parameters to bioprint 3D constructs, *is identifying* appropriate materials to dispense. Therefore, a number of characteristics must be considered. First and foremost, the effect of the *bioprinted* material *and material processing* on cell viability and behavior must be investigated. Selected materials should maintain or induce desired functions of incorporated cells. *Pilot studies ensuring biocompatibility prior to bioprinting may be warranted.* Material components, including additives (such as cross-linking [42] and gelling agents [39]) or environmental conditions (UV exposure [43], humidity and temperature [40]) that may be required to achieve desired material properties should be tested to ensure cell behavior is maintained. *If directly printing cells within a 3D architecture*, typical scaffold processing such as critical point drying [44], polymers that require toxic solvents [45], extruded thermoplastics [46], and powder-binder-based systems [47] should be avoided. Selected structural materials should also have a viscosity that is compatible with the printing system. For biological materials, agarose [39], alginate [8,38], collagen type I [8], and Pluronic F127 [40] have been successfully organized into micro- and macroscale patterns with and without suspended cells. All of these polymer systems have been shown to maintain high cell viability when cultured *in vitro.*

We have focused our recent work on two temperature-sensitive hydrogels, Pluronic F127 and collagen type I [8,40]. This combination of materials was selected for a number of reasons. First, Pluronic F127 has been used as a delivery vehicle in a number of cardiovascular applications [48–51]. It also serves as an excellent bioprinting material due to its biocompatibility, reversible temperature-sensitive gelling between 10–40°C, adhesion to surfaces, and broad range of viscosities at room temperature [52,53]. F127 (40wt%), when printed at room temperature, maintains its high viscosity state long enough for adjacent 4°C collagen volumes to gel. Moreover, F127 is easily rinsed away after printing (if desired). Collagen I (3mg/mL) was selected as our biomaterial for its outstanding *in vitro* and *in vivo* compatibility with cellular and microvascular [9,54–59] and cardiovascular experimental systems [60,61].

Work Area and Equipment Considerations

In order to successfully fabricate tissue constructs for experimental use, a number of environmental factors and equipment characteristics should be considered. A major concern is the maintenance of a sterile work area and preventing sample contamination while printing. The size of some bioprinters [32] may permit operation within a biosafety hood. Larger commercial systems offer the option of environmental isolation and permit the addition of HEPA filters and laminar flow capabilities to minimize work area contamination [40]. Bioprinter components, particularly instrumentation in direct contact with construct materials, should be designed for compatibility with standard sterilization techniques. In our BAT system, we utilize commercially available components (syringes, pistons, connectors, and needles) compatible with autoclave or ethylene oxide sterilization prior to use. When possible, disposable components (particularly needles and syringes) are used to minimize opportunities for sample contamination.

Bioprinter components must also be compatible with printing conditions. Due to the small volumes and high surface-to-volume ratios of printed patterns, we have found temperature and humidity play important roles in maintaining construct fidelity and viability[40]. Due to the major role of computer controls within bioprinting devices, care should be taken to isolate moisture and temperature sensitive components from the main printing system compartment.

The printing surface plays an important role in engineered construct fabrication. To date, many substrate considerations for bioprinting have focused on surface-material wetting [8]. The printing substrate, typically polymer films, gel coated polymer sheets, or petri dishes have been used solely as a stage for physical support of dispensed materials or as degradable material permitting stacking of printed layers [9,32,34,37,39–41,45,62,63]. We see the printing substrate as an opportunity to add structural integrity and facilitate transport and subsequent implantation. Currently, most printed constructs are on the order of a few hundred microns thick. Moreover, due to fabrication from low concentration alginates and collagen, these thin volumes are not conducive to handling and transport. Therefore, we have been begun printing directly onto more substantial materials, such as polymer screens and electrospun scaffolds. Electrospinning permits control over scaffold components, such as fiber size, orientation, porosity, and resulting mechanical properties [64–66]. We can engineer these surfaces to provide a number of key benefits, such as:

- **a.** scaffold porosity to facilitate construct incorporation, preventing interface delamination after printing
- **b.** mechanical strength to permit construct-scaffold composite transport for *in vitro* conditioning and incorporation into bioreactor systems
- **c.** facilitate transport to implantation site and provide compatibility with suturing techniques
- **d.** scaffold materials may be designed to direct construct-host interaction once an engineered construct is implanted.

Direct-write Printing Parameters

Precise deposition of biomaterials begins with the method of dispensing. There are currently three primary methods to direct-write materials onto a substrate, pneumatic [8,37,40,41], mechanical [8,32,38–40], and pneumatic-mechanical hybrid powered dispensing systems [8,40]. In our experience, pneumatic systems are more suited to dispensing high viscosity materials while mechanical systems facilitate dispensing low viscosity materials.

As described above, hydrogels have been the material of choice for direct-write bioprinting. As these materials are dispensed onto a surface, two main material properties affect the printed line, viscosity and surface wetting [8]. Viscosity, depending on the hydrogel, may be a function of a number of factors, including mechanism of gelling, polymer-solvent miscibility, polymer molecular weight, polymer concentration, temperature, cross-linker activity, and humidity [67]. Surface wetting will be mostly determined by the interfacial energies associated with the surface and substrate interfaces of the printed material [67]. In addition to material properties, four device controlled variables will determine the physical dimensions of a bioprinted line; needle diameter, material flow rate, printed line height (the distance from the surface to the needle opening), and linear write speed.

Before printing any material, it is important to consider all of the abovementioned properties. We suggest minimizing the number of printing variables by first determining the optimum conditions required to maintain a material's viscosity. For example, maintaining 25wt% F127 dissolved in phosphate buffered saline at room temperature yields a viscosity of approximately 30 mPa*s. Once the hydrogel viscosity is stable, printing parameters from run to run will be more reproducible.

To assist others in the direct-write bioprinting of hydrogels, we have assembled the following tables (Table 2 and 3). These tables offer example printing parameters for relatively low, medium, high, and very high viscosity hydrogels utilizing two dispensing methods, pneumatic and mechanical. For these examples, we have printed a widely used, temperature-sensitive hydrogel, Pluronic F127. In both dispensing systems, commercially available "general purpose pistons" (Nordson EFD, East Providence, RI), 5cc barrels (Nordson EFD, East Providence, RI), and syringe needles (McMaster-Carr, Elmhurst, IL) were used. All components were autoclaved or ethylene oxide sterilized prior to use.

In each table, linear write speed was held constant at 3mm/s across all samples. The required dispensing value (line pressure or piston displacement rate) for three standard needle sizes, line height, and resulting line widths for each material are presented. In general, as material viscosity increases and needle diameter decreases, greater force is required to dispense the material. Likewise, as needle diameter decreases, smaller volumes of material are dispensed, resulting in reduced line height and diameter.

Pattern Design Considerations

From a pattern design perspective, the line width and height of a dispensed material may be critical. For our purposes, these characteristics are essential to reproducibly fabricate experimental constructs. A line height is determined based on the needle size, material flow rate, and linear write speed. Three typical variable combinations occur while printing. 1) If all three aforementioned variables are balanced (Figure 3a), the leading edge of the printed hydrogel will be even with the needle. This situation yields relatively uniform lines and high pattern fidelity in-plane and for subsequent layers. 2) If the write speed is too low, the flow rate too high, or line height is too small, a material bulge will be seen leading the front edge of the needle (Figure 3b). In this scenario, line widths increase, in-plane pattern fidelity is still maintained but added layers may compress or distort lower layers. 3) If write speed is too high, flow rate to low, or line height is too high, the hydrogel may lag behind the needle, often characterized by a gap between the hydrogel and the printing surface (Figure 3c). This situation leads to poor pattern fidelity in-plane and in multiple layers. In particular, precise corners and inter-plane alignment of features are difficult to achieve.

Once the parameters for a uniform line are determined, more complex patterns may be designed. When possible, we design patterns as a single continuous dispensed line. Continuous lines lead to more uniform line characteristics (dispensed line height and width),

facilitating in-plane feature design and the fidelity required to dispense additional layers. Utilizing 40wt% F127, we have printed continuous patterns greater than 15 layers thick without any noticeable vertical deformation. An example hollow diamond pattern is presented (Figure 3d). This pattern takes advantage of the high viscosity and adhesion of room temperature 40wt% F127. *No additional cross-linking agents or chemical additives were added.* Concentric squares of greater (Figure 3e) and then smaller (Figure 3f) width were continuously dispensed until the pattern was eventually capped (Figure 3g). Each layer may be off-set as much as 1/2 the line width in the x- and y- direction from the previous layer. *A unique feature of this geometry is a lack of external support for the middle layers of the structure. The base layer (1.4mm × 1.4mm) is significantly smaller than the widest layer (5mm × 5mm).* The finished pattern, *14 layers tall*, is a freestanding hollow diamond approximately 5.6mm in height (Figure 3h).

In past work, we have found it difficult to maintain pattern resolution with low viscosity materials, line width was greatly affected by the substrate material and ambient humidity [40]. As a result, line width was highly variable and adjacent dispensed lines tended to contact each other. These issues became more problematic when attempting to print multiple layers. As a result, we have focused our recent pattern designs on a two material mold and fill system – printing a high viscosity structural material mold followed by a low viscosity biological material that fills in the spaces. A simple mold and fill pattern is presented in Figure 4.

In our mold and fill system, the high viscosity material serves a number of purposes. First, it provides structural integrity for the printed pattern. The high viscosity gel *is used to form inner and outer walls o the fabricated constructs. In our experiments, we have found F127* constrains the low viscosity material as it polymerizes, defining its dimensions. In this manner, low viscosity materials may be formed into complex shapes of nearly any thickness. In addition, this printing strategy permits compartmentalization of engineered tissues. If desired, cells types may be isolated or mixed in controlled volumes for *in vitro* culture or *in vivo* use. Internal “walls” are easily modified to control the proximity of each internal feature.

As fabricated structures increase in complexity and size, a major concern is the incorporation of support structures within the fabricated pattern. Appropriate patterns and materials must be selected. Higher viscosity hydrogels should be utilized for use as structural components. Pilot experiments should be conducted to evaluate material performance. For instance, a series of hydrogel lines could be printed at specified inter-line distances (Figure 5a). A second layer of perpendicular lines could be printed to determine the maximum distance the material can span between supports. For example, we have found 300μm thick lines of 40wt% F127 may span approximately 3mm with minimal vertical deformation (Figure 5b). In external walls, we have found straight sections printed with 40wt% F127 with widths less than 300μm and lengths greater than 5 or 6mm often buckle, particularly if the patterns are exposed to a low humidity environment for extended time. We address these issues by fabricating thicker walls, by designing patterns with external supports every 5 or 6mm, and placing printed patterns in a humid incubators as soon as possible (Figure 5c–d) [40].

A support strategy that may be used within various patterns is the use of walls defining internal features as supports for successive layers. For example, if forming a pattern with multiple converging microchannels (Figure 5e–f), walls can be used as supports for alternating short perpendicular lines to enclose the channel (if the channel width is too wide for the selected material to span, support posts or lines may need to be printed within the channel). Once enclosed, these channel tops may be used as the base for successive printed

layers (Figure 5g). If a combination of low and high viscosity materials are used, it is crucial that the high viscosity material maintains viscosity when contacting the other material(s) (Figure 5h), particularly if time is required for the low-viscosity material to gel (Figure 5i).

An additional variable to consider while designing and fabricating larger structures is time. The time required to prepare hydrogels and solutions, to achieve and maintain optimal temperatures, chemical or thermal gelling times, and bioprinting environmental conditions should all be considered when designing a construct. While printing, extended periods of time exposed to non-optimal temperatures or humidity negatively affect both material properties [40] and cell viability [68]. For example, a converging microchannel pattern (Figure 5f) takes approximately 5min. Once finished, there are no noticeable distortions. However, if printing serial patterns within the same petri dish, pattern distortions, particularly in long and thin external features begin to appear (Figure 5g). As patterns become larger (such as the 3 tiered pattern requiring 15 minutes), pattern distortion may become a major concern. In these situations, it may be beneficial to separate print runs and place patterns into incubators immediately after completion.

Future Directions

The current state-of-the-art bioprinted constructs are still relatively thin layers of cells within a biological hydrogel [23,32,40,62,69]. Although still in its infancy, the technology has provided a method to arrange biological materials into planar and 3D shapes. However, these structures are very simple – containing one or two cell types within a few select matrix proteins. In order to achieve true tissue construction, a number of obstacles will have to be overcome.

The major hurdle preventing the development of larger regenerative tissues, is the lack of an invested microvasculature [30]. Without a functional circulatory system, the potential size of engineered constructs will be diffusion limited to a few hundred microns. A widely used method of construct vascularization relies on infiltration of host microvessels into an implanted construct [70,71]. Although 3D scaffolds have been printed with angiogenesis inducing materials [72], this printing strategy lacks specificity and control of microvessel development. Invading microvessels have a limited penetration depth, and therefore, prevent the successful incorporation of larger constructs. In addition, these vessels, while migrating and developing within the implanted structure, may distort or destroy regions of the engineered tissue. From a design standpoint, it would be preferred to fabricate a compartmentalized tissue with regions or materials that preferentially direct vessel in-growth or, ideally, build a construct with the microvasculature in place before implantation. *Initial experiments have been conducted, providing evidence of microvascular cell and microvessel fragments incorporation into in vitro 3D scaffolds (*Figure 4). In vivo evaluation of these constructs will further elucidate bioprinting modifications that may be required for the fabrication of future engineered constructs.

In addition to complex microvessel networks, native tissues contain unique cellular combinations and organization. Similarly, unique extracellular matrix combinations and organization are present in each tissue. *New techniques will need to be developed to mimic these complex biological structures. Ideally, future regenerative therapies will closely mimic the structure and biology of a diseased target site. Future scientists* will need to determine which types and combinations of cells and matrix are required to drive tissue recovery or tissue replacement.

In our opinion, the capability of bioprinting to dispense different cell-matrix systems in multiple 3D shapes onto various scaffold materials provides a significant tool for future investigations of cell-matrix-host regenerative therapies. *Current systems may be used to*

design and fabricate a variety of in vitro systems for evaluating cell behavior and interactions. With true 3D control of cell placement, unique models for studying cell migration and proliferation may be fabricated. A multi-needle system could print alternating lines, planes, or other geometric shapes of cells within or around individual or multiple cell populations. This could be expanded for in vitro evaluation of bioprinted cell interations within or around excised tissue samples or modified extracellular matrices. In addition, structural materials may be doped with any number of natural or synthetic factors to affect the surrounding biological behavior. These characteristics may provide researchers with endless opportunities for designing engineered tissues or custom systems for experimental evaluation of biological factors (such as cell signals and growth factors). Bioprinting also provides a unique platform for pharmaceutical agent evaluation. Matrix materials or applied hydrogels could be arranged to establish designed gradients in precise proximity to individual or multiple cells within a 3D volume. Microliters to picoliters of a desired experimental drug could be evaluated within a designed bioprinted structure.

As discussed previously, current bioprinting strategies rely on dispensing materials onto a surface to build 3D structures from the bottom up. As future structures become more complicated, this method of printing may be inadequate. An alternative method, and capability unique to direct-write bioprinting, is the controlled dispensing of materials within a volume (Figure 6a). In theory, this bioprinting strategy would permit 3D deposition of materials from any angle into any position within a volume on any plane. It would also facilitate precise positioning and mixing of small volumes of different matrices and matrix-cell suspensions. Initial experiments evaluating “in-matrix” bioprinting of cell-matrix suspensions have been conducted (Figure 6b-f). In these examples, microvascular cell-collagen and microvessel fragment-collagen bioinks were dispensed within a larger volume of collagen. In preliminary results, simple lines of cells remain viable after printing, forming cord-like morphologies within one day. Over five days of culture, cells migrate throughout the construct volume, suggesting this may be a viable method for organizing and delivering cells for future regenerative therapies.

We believe biological printing, or bioprinting, will be a key technology for fabricating future regenerative therapies, devices, and engineered tissues. With the aforementioned issues in mind, *researchers* are far from fabricating true artificial tissues or tissue analogs. However, *investigators* are poised to begin forming more complex hydrogel and cell-based regenerative therapies for experimental investigation. *Researchers* have begun to develop baseline technologies that are laying the foundation for these systems. Groups are working with a number of biohybrid systems for dispensing drugs and biological factors to target tissues [3,16,18,27,51,68,73,74]. Researchers are beginning to fabricate 3D structures with multiple cell types, including fibroblasts [8,39,75], smooth muscle cells [39], endothelial cells [8,40], and neural cells [76]. As this work progresses, printing conditions, techniques, and methodologies may be combined to fabricate complex composite systems that more closely mimic physiological structures. By providing the above foundational bioprinting information and considerations, we hope to make this technology more accessible to new researchers and accelerate efforts to bioprint future biohybrid systems and regenerative therapies for a wide range of biomedical applications.

Acknowledgments

Funding was provided by the National Institutes of Health, grant R01EB007556.

References

1. Lysaght MJ, Crager J. Origins. Tissue Eng Part A. 2009; 15(7):1449–50. [PubMed: 19327019]

2. Brown P. Abdominal wall reconstruction using biological tissue grafts. AORN J. 2009; 90(4):513–20. quiz 521–4. [PubMed: 19860033]
3. Schmidt JJ, Rowley J, Kong HJ. Hydrogels used for cell-based drug delivery. J Biomed Mater Res A. 2008; 87(4):1113–22. [PubMed: 18837425]
4. Esaki J, Marui A, Tabata Y, Komeda M. Controlled release systems of angiogenic growth factors for cardiovascular diseases. Expert Opin Drug Deliv. 2007; 4(6):635–49. [PubMed: 17970666]
5. Macchiarini P, Jungebluth P, Go T, Asnaghi MA, Rees LE, Cogan TA, Dodson A, Martorell J, Bellini S, Parnigotto PP, et al. Clinical transplantation of a tissue-engineered airway. Lancet. 2008; 372(9655):2023–30. [PubMed: 19022496]
6. Atala A, Bauer SB, Soker S, Yoo JJ, Retik AB. Tissue-engineered autologous bladders for patients needing cystoplasty. Lancet. 2006; 367(9518):1241–6. [PubMed: 16631879]
7. Llames S, Garcia E, Garcia V, del Rio M, Larcher F, Jorcano JL, Lopez E, Holguin P, Miralles F, Otero J, et al. Clinical results of an autologous engineered skin. Cell Tissue Bank. 2006; 7(1):47–53. [PubMed: 16511664]
8. Smith CM, Stone AL, Parkhill RL, Stewart RL, Simpkins MW, Kachurin AM, Warren WL, Williams SK. Three-dimensional bioassembly tool for generating viable tissue-engineered constructs. Tissue Eng. 2004; 10(9–10):1566–76. [PubMed: 15588416]
9. Chang CC, Hoying JB. Directed three-dimensional growth of microvascular cells and isolated microvessel fragments. Cell Transplant. 2006; 15(6):533–40. [PubMed: 17121164]
10. Dos Reis G, Fenili F, Gianfelice A, Bongiorno G, Marchesi D, Scopelliti PE, Borgonovo A, Podesta A, Indrieri M, Ranucci E, et al. Direct Microfabrication of Topographical and Chemical Cues for the Guided Growth of Neural Cell Networks on Polyamidoamine Hydrogels. Macromol Biosci. 2010
11. Wang S, Wong Po Foo C, Warrier A, Poo MM, Heilshorn SC, Zhang X. Gradient lithography of engineered proteins to fabricate 2D and 3D cell culture microenvironments. Biomed Microdevices. 2009
12. Kane RS, Takayama S, Ostuni E, Ingber DE, Whitesides GM. Patterning proteins and cells using soft lithography. Biomaterials. 1999; 20(23–24):2363–76. [PubMed: 10614942]
13. Cimetta E, Pizzato S, Bollini S, Serena E, De Coppi P, Elvassore N. Production of arrays of cardiac and skeletal muscle myofibers by micropatterning techniques on a soft substrate. Biomed Microdevices. 2009; 11(2):389–400. [PubMed: 18987976]
14. Trkov S, Eng G, Di Liddo R, Parnigotto PP, Vunjak-Novakovic G. Micropatterned three-dimensional hydrogel system to study human endothelial-mesenchymal stem cell interactions. J Tissue Eng Regen Med. 2010; 4(3):205–15. [PubMed: 19998330]
15. Sobral JM, Caridade SG, Sousa RA, Mano JF, Reis RL. Three-dimensional plotted scaffolds with controlled pore size gradients: Effect of scaffold geometry on mechanical performance and cell seeding efficiency. Acta Biomater. 2010
16. Park SA, Lee SH, Kim WD. Fabrication of porous polycaprolactone/hydroxyapatite (PCL/HA) blend scaffolds using a 3D plotting system for bone tissue engineering. Bioprocess Biosyst Eng. 2010
17. Duan B, Wang M, Zhou WY, Cheung WL, Li ZY, Lu WW. Three-dimensional nanocomposite scaffolds fabricated via selective laser sintering for bone tissue engineering. Acta Biomater. 2010; 6(12):4495–505. [PubMed: 20601244]
18. Mondy WL, Cameron D, Timmermans JP, De Clerck N, Sasov A, Casteleyn C, Piegl LA. Micro-CT of corrosion casts for use in the computer-aided design of microvasculature. Tissue Eng Part C Methods. 2009; 15(4):729–38. [PubMed: 19290799]
19. Lan PX, Lee JW, Seol YJ, Cho DW. Development of 3D PPF/DEF scaffolds using micro-stereolithography and surface modification. J Mater Sci Mater Med. 2009; 20(1):271–9. [PubMed: 18763023]
20. Wilson WC Jr, Boland T. Cell and organ printing 1: protein and cell printers. Anat Rec A Discov Mol Cell Evol Biol. 2003; 272(2):491–6. [PubMed: 12740942]
21. Madou, MJ. Fundamentals of microfabrication : the science of miniaturization. Boca Raton: CRC Press; 2002. p. 723

22. Tan W, Desai TA. Microscale multilayer cocultures for biomimetic blood vessels. J Biomed Mater Res A. 2005; 72(2):146–60. [PubMed: 15558555]
23. Mata A, Kim EJ, Boehm CA, Fleischman AJ, Muschler GF, Roy S. A three-dimensional scaffold with precise micro-architecture and surface micro-textures. Biomaterials. 2009; 30(27):4610–7. [PubMed: 19524292]
24. Zamanian B, Masaeli M, Nichol JW, Khabiry M, Hancock MJ, Bae H, Khademhosseini A. Interface-directed self-assembly of cell-laden microgels. Small. 2010; 6(8):937–44. [PubMed: 20358531]
25. Shah RK, Kim JW, Weitz DA. Monodisperse stimuli-responsive colloidosomes by self-assembly of microgels in droplets. Langmuir. 2010; 26(3):1561–5. [PubMed: 19950936]
26. Du Y, Ghodousi M, Lo E, Vidula MK, Emiroglu O, Khademhosseini A. Surface-directed assembly of cell-laden microgels. Biotechnol Bioeng. 2010; 105(3):655–62. [PubMed: 19777588]
27. Li MG, Tian XY, Chen XB. A brief review of dispensing-based rapid prototyping techniques in tissue scaffold fabrication: role of modeling on scaffold properties prediction. Biofabrication. 2009; 1(3):032001. [PubMed: 20811104]
28. Herath HM, Di Silvio L, Evans JR. Biological evaluation of solid freeformed, hard tissue scaffolds for orthopedic applications. J Appl Biomater Biomech. 2010; 8(2):89–96. [PubMed: 20740471]
29. Nielson R, Kaehr B, Shear JB. Microreplication and design of biological architectures using dynamic-mask multiphoton lithography. Small. 2009; 5(1):120–5. [PubMed: 19040218]
30. Lokmic Z, Mitchell GM. Engineering the microcirculation. Tissue Eng Part B Rev. 2008; 14(1): 87–103. [PubMed: 18454636]
31. Xu T, Jin J, Gregory C, Hickman JJ, Boland T. Inkjet printing of viable mammalian cells. Biomaterials. 2005; 26(1):93–9. [PubMed: 15193884]
32. Mironov V, Visconti RP, Kasyanov V, Forgacs G, Drake CJ, Markwald RR. Organ printing: tissue spheroids as building blocks. Biomaterials. 2009; 30(12):2164–74. [PubMed: 19176247]
33. Guillemot F, Souquet A, Catros S, Guillotin B, Lopez J, Faucon M, Pippenger B, Bareille R, Remy M, Bellance S, et al. High-throughput laser printing of cells and biomaterials for tissue engineering. Acta Biomater. 2009
34. Jakab K, Damon B, Neagu A, Kachurin A, Forgacs G. Three-dimensional tissue constructs built by bioprinting. Biorheology. 2006; 43(3–4):509–13. [PubMed: 16912422]
35. Jang D, Kim D, Moon J. Influence of fluid physical properties on ink-jet printability. Langmuir. 2009; 25(5):2629–35. [PubMed: 19437746]
36. Khan MS, Fon D, Li X, Tian J, Forsythe J, Garnier G, Shen W. Biosurface engineering through ink jet printing. Colloids Surf B Biointerfaces. 2010; 75(2):441–7. [PubMed: 19879112]
37. Chang R, Nam J, Sun W. Effects of Dispensing Pressure and Nozzle Diameter on Cell Survival from Solid Freeform Fabrication-Based Direct Cell Writing. Tissue Eng. 2007
38. Cohen DL, Malone E, Lipson H, Bonassar LJ. Direct freeform fabrication of seeded hydrogels in arbitrary geometries. Tissue Eng. 2006; 12(5):1325–35. [PubMed: 16771645]
39. Norotte C, Marga FS, Niklason LE, Forgacs G. Scaffold-free vascular tissue engineering using bioprinting. Biomaterials. 2009; 30(30):5910–7. [PubMed: 19664819]
40. Smith CM, Christian JJ, Warren WL, Williams SK. Characterizing environmental factors that impact the viability of tissue-engineered constructs fabricated by a direct-write bioassembly tool. Tissue Eng. 2007; 13(2):373–83. [PubMed: 17518570]
41. Lee W, Lee V, Polio S, Keegan P, Lee JH, Fischer K, Park JK, Yoo SS. On-demand three-dimensional freeform fabrication of multi-layered hydrogel scaffold with fluidic channels. Biotechnol Bioeng. 2010; 105(6):1178–86. [PubMed: 19953677]
42. Sabnis A, Rahimi M, Chapman C, Nguyen KT. Cytocompatibility studies of an in situ photopolymerized thermoresponsive hydrogel nanoparticle system using human aortic smooth muscle cells. J Biomed Mater Res A. 2009; 91(1):52–9. [PubMed: 18690661]
43. Bryant SJ, Nuttelman CR, Anseth KS. Cytocompatibility of UV and visible light photoinitiating systems on cultured NIH/3T3 fibroblasts in vitro. J Biomater Sci Polym Ed. 2000; 11(5):439–57. [PubMed: 10896041]

44. Sachlos E, Reis N, Ainsley C, Derby B, Czernuszka JT. Novel collagen scaffolds with predefined internal morphology made by solid freeform fabrication. Biomaterials. 2003; 24(8):1487–97. [PubMed: 12527290]
45. Lee M, Dunn JC, Wu BM. Scaffold fabrication by indirect three-dimensional printing. Biomaterials. 2005; 26(20):4281–9. [PubMed: 15683652]
46. Mondrinos MJ, Dembzynski R, Lu L, Byrapogu VK, Wootton DM, Lelkes PI, Zhou J. Porogen-based solid freeform fabrication of polycaprolactone-calcium phosphate scaffolds for tissue engineering. Biomaterials. 2006; 27(25):4399–408. [PubMed: 16678255]
47. Shanjani Y, De Croos JN, Pilliar RM, Kandel RA, Toyserkani E. Solid freeform fabrication and characterization of porous calcium polyphosphate structures for tissue engineering purposes. J Biomed Mater Res B Appl Biomater. 2010; 93(2):510–9. [PubMed: 20162726]
48. Namgung R, Nam S, Kim SK, Son S, Singha K, Kwon JS, Ahn Y, Jeong MH, Park IK, Garripelli VK, et al. An acid-labile temperature-responsive sol-gel reversible polymer for enhanced gene delivery to the myocardium and skeletal muscle cells. Biomaterials. 2009; 30(28):5225–33. [PubMed: 19552951]
49. Oh KS, Song JY, Yoon SJ, Park Y, Kim D, Yuk SH. Temperature-induced gel formation of core/shell nanoparticles for the regeneration of ischemic heart. J Control Release. 2010
50. Zou Y, Qi Y, Roztocil E, Davies MG. Patterns of gelatinase activation induced by injury in the murine femoral artery. J Surg Res. 2009; 154(1):135–42. [PubMed: 19101695]
51. Yoon JJ, Chung HJ, Park TG. Photo-crosslinkable and biodegradable Pluronic/heparin hydrogels for local and sustained delivery of angiogenic growth factor. J Biomed Mater Res A. 2007; 83(3): 597–605. [PubMed: 17503533]
52. Escobar-Chavez JJ, Lopez-Cervantes M, Naik A, Kalia YN, Quintanar-Guerrero D, Ganem-Quintanar A. Applications of thermo-reversible pluronic F-127 gels in pharmaceutical formulations. J Pharm Pharm Sci. 2006; 9(3):339–58. [PubMed: 17207417]
53. Ruel-Gariepy E, Leroux JC. In situ-forming hydrogels--review of temperature-sensitive systems. Eur J Pharm Biopharm. 2004; 58(2):409–26. [PubMed: 15296964]
54. Chang CC, Nunes SS, Sibole SC, Krishnan L, Williams SK, Weiss JA, Hoying JB. Angiogenesis in a microvascular construct for transplantation depends on the method of chamber circulation. Tissue Eng Part A. 2010; 16(3):795–805. [PubMed: 19778185]
55. Shepherd BR, Chen HY, Smith CM, Gruionu G, Williams SK, Hoying JB. Rapid perfusion and network remodeling in a microvascular construct after implantation. Arterioscler Thromb Vasc Biol. 2004; 24(5):898–904. [PubMed: 14988090]
56. Ashley RA, Dubuque SH, Dvorak B, Woodward SS, Williams SK, Kling PJ. Erythropoietin stimulates vasculogenesis in neonatal rat mesenteric microvascular endothelial cells. Pediatr Res. 2002; 51(4):472–8. [PubMed: 11919332]
57. Hoying JB, Williams SK. Effects of basic fibroblast growth factor on human microvessel endothelial cell migration on collagen I correlates inversely with adhesion and is cell density dependent. J Cell Physiol. 1996; 168(2):294–304. [PubMed: 8707865]
58. Hoying JB, Boswell CA, Williams SK. Angiogenic potential of microvessel fragments established in three-dimensional collagen gels. In Vitro Cell Dev Biol Anim. 1996; 32(7):409–19. [PubMed: 8856341]
59. Pratt KJ, Jarrell BE, Williams SK, Carabasi RA, Rupnick MA, Hubbard FA. Kinetics of endothelial cell-surface attachment forces. J Vasc Surg. 1988; 7(4):591–9. [PubMed: 3352078]
60. Giraud MN, Ayuni E, Cook S, Siepe M, Carrel TP, Tevaearai HT. Hydrogel-based engineered skeletal muscle grafts normalize heart function early after myocardial infarction. Artif Organs. 2008; 32(9):692–700. [PubMed: 18684206]
61. Clause KC, Tinney JP, Liu LJ, Keller BB, Tobita K. Engineered early embryonic cardiac tissue increases cardiomyocyte proliferation by cyclic mechanical stretch via p38-MAP kinase phosphorylation. Tissue Eng Part A. 2009; 15(6):1373–80. [PubMed: 19196150]
62. Jakab K, Norotte C, Damon B, Marga F, Neagu A, Besch-Williford CL, Kachurin A, Church KH, Park H, Mironov V, et al. Tissue engineering by self-assembly of cells printed into topologically defined structures. Tissue Eng Part A. 2008; 14(3):413–21. [PubMed: 18333793]

63. Dellinger JG, Cesarano J 3rd, Jamison RD. Robotic deposition of model hydroxyapatite scaffolds with multiple architectures and multiscale porosity for bone tissue engineering. J Biomed Mater Res A. 2007; 82(2):383–94. [PubMed: 17295231]
64. Boland ED, Matthews JA, Pawlowski KJ, Simpson DG, Wnek GE, Bowlin GL. Electrospinning collagen and elastin: preliminary vascular tissue engineering. Front Biosci. 2004; 9:1422–32. [PubMed: 14977557]
65. McManus MC, Boland ED, Koo HP, Barnes CP, Pawlowski KJ, Wnek GE, Simpson DG, Bowlin GL. Mechanical properties of electrospun fibrinogen structures. Acta Biomater. 2006; 2(1):19–28. [PubMed: 16701855]
66. McManus MC, Boland ED, Simpson DG, Barnes CP, Bowlin GL. Electrospun fibrinogen: feasibility as a tissue engineering scaffold in a rat cell culture model. J Biomed Mater Res A. 2007; 81(2):299–309. [PubMed: 17120217]
67. Sperling, LH. Introduction to physical polymer science. Vol. xxvii. New York: Wiley; 1992. p. 594
68. Pepper ME, Cass CA, Mattimore JP, Burg T, Booth BW, Burg KJ, Groff RE. Post-bioprinting processing methods to improve cell viability and pattern fidelity in heterogeneous tissue test systems. Conf Proc IEEE Eng Med Biol Soc. 2010; 1:259–62. [PubMed: 21096750]
69. Fernandez JG, Mills CA, Martinez E, Lopez-Bosque MJ, Sisquella X, Errachid A, Samitier J. Micro- and nanostructuring of freestanding, biodegradable, thin sheets of chitosan via soft lithography. J Biomed Mater Res A. 2008; 85(1):242–7. [PubMed: 17688270]
70. Laschke MW, Vollmar B, Menger MD. Inosculation: connecting the life-sustaining pipelines. Tissue Eng Part B Rev. 2009; 15(4):455–65. [PubMed: 19552605]
71. Borselli C, Ungaro F, Oliviero O, d'Angelo I, Quaglia F, La Rotonda MI, Netti PA. Bioactivation of collagen matrices through sustained VEGF release from PLGA microspheres. J Biomed Mater Res A. 2010; 92(1):94–102. [PubMed: 19165799]
72. Barralet J, Gbureck U, Habibovic P, Vorndran E, Gerard C, Doillon CJ. Angiogenesis in calcium phosphate scaffolds by inorganic copper ion release. Tissue Eng Part A. 2009; 15(7):1601–9. [PubMed: 19182977]
73. Jay SM, Shepherd BR, Andrejecsk JW, Kyriakides TR, Pober JS, Saltzman WM. Dual delivery of VEGF and MCP-1 to support endothelial cell transplantation for therapeutic vascularization. Biomaterials. 2010; 31(11):3054–62. [PubMed: 20110124]
74. Singh A, Suri S, Roy K. In-situ crosslinking hydrogels for combinatorial delivery of chemokines and siRNA-DNA carrying microparticles to dendritic cells. Biomaterials. 2009; 30(28):5187–200. [PubMed: 19560815]
75. Skardal A, Zhang J, Prestwich GD. Bioprinting vessel-like constructs using hyaluronan hydrogels crosslinked with tetrahedral polyethylene glycol tetracrylates. Biomaterials. 2010; 31(24):6173–81. [PubMed: 20546891]
76. Lee W, Pinckney J, Lee V, Lee JH, Fischer K, Polio S, Park JK, Yoo SS. Three-dimensional bioprinting of rat embryonic neural cells. Neuroreport. 2009; 20(8):798–803. [PubMed: 19369905]

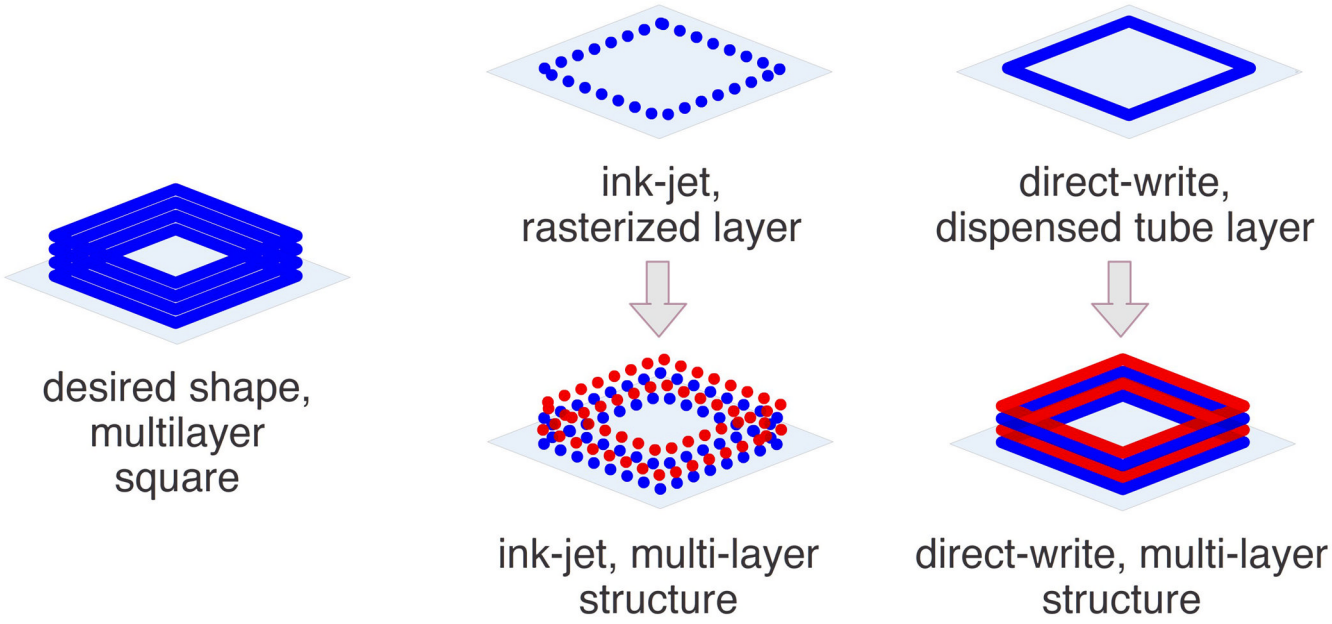

Figure 1.
Illustration comparing ink-jet and direct-write bioprinting of a 3D construct. Alternating layer colors help illustrate multiple layer construction. Depending on desired design and device capabilities, each layer may be composed of unique or identical materials.

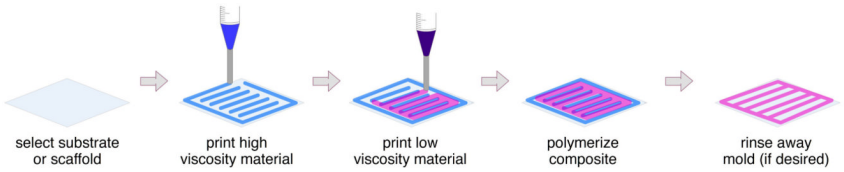

Figure 2.
Illustration of two material “mold and fill” direct-write printing fabrication strategy.

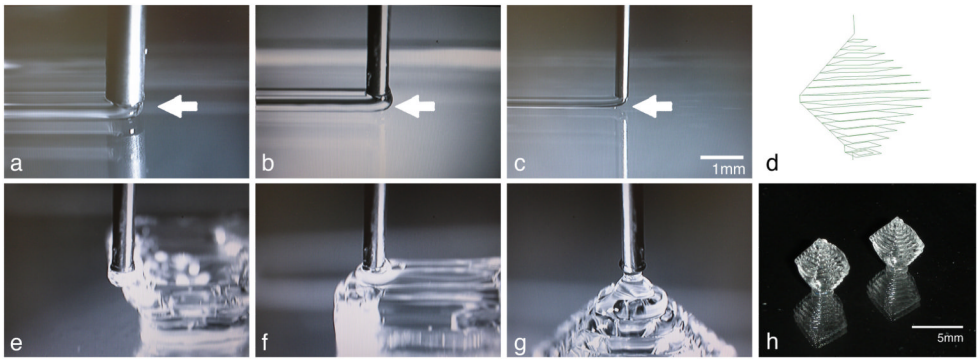

Figure 3.

Images of 40wt% F127 lines printed onto a petri dish from a 20ga(a), 25ga(b), and 30ga(c) needle. Arrows point to the leading edge of each printed line. Once line width and height are determined, *desired* 3D shapes can be printed. d) Pattern line path of a hollow diamond pattern composed of concentric squares. e-h) Images of the printed pattern. Scale bar for a-c and e-g is 1mm.

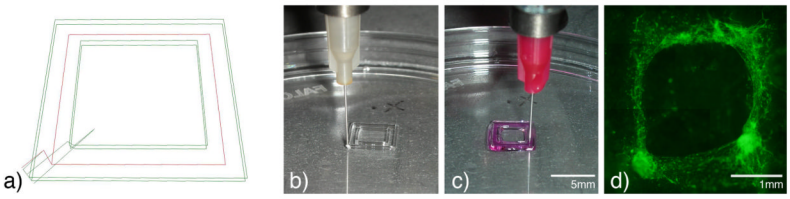

Figure 4.
Example of simple two-material direct-write printed pattern. a) Line path representing printed high viscosity material (green) and low viscosity material (red). Actual images of bioprinted high viscosity 40wt% Pluronic F127 (b) followed by low viscosity collagen with suspended microvascular cells and microvesesl fragments (c). After 7 days of culture, cells and fragments (green) form neovascular networks within the patterned collagen (d).

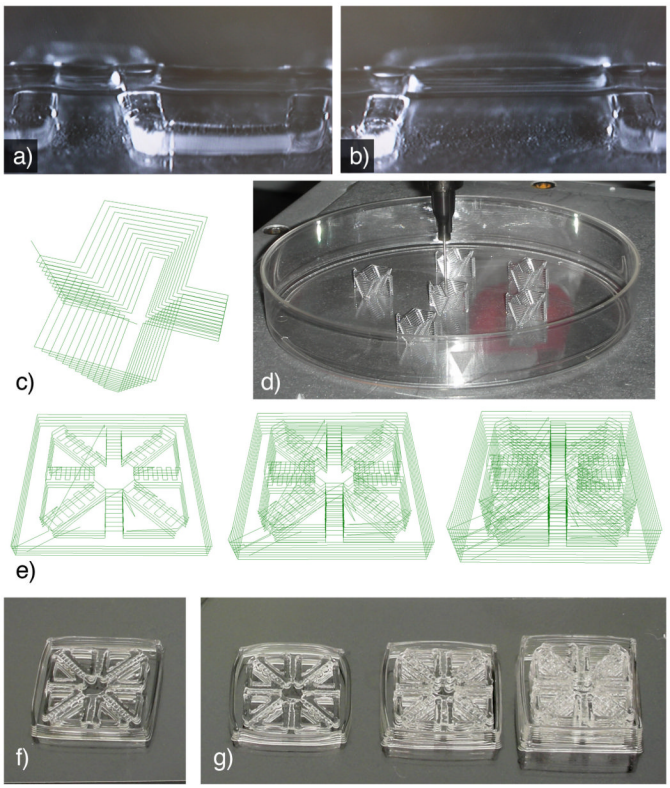

Figure 5.

Examples of bioprinted structures. Images of 40wt% F127 bioprinted in 300μm widths for evaluating inter-line distance effect on subsequent layer deposition. a) The base F127 layer is composed of lines spaced 1.5mm and 2.5mm apart, resulting in a second line of F127 spanning respective gaps of 1mm and 2mm. b) Base lines spaced 3.5mm apart, with a 3mm gap may also be spanned by dispensed F127. Scale bar for a and b = 1mm. c) An example wedge mold with exterior wall supports on the long (11mm) sides. d) Images of printed 40wt% F127 wedge molds. e) Line paths of modular pattern containing converging 500μm microchannels. Each outer edge of the microchannel pattern is 14.4mm. These examples show an individual channel pattern and two and three patterns stacked on top of each other. As patterns are stacked, the top layer of each module was designed to become the base support for the next module. f) Image of printed microchannel pattern module immediately after printing. g) Distortions in the outer walls of printed modules are visible in the single, double, and triple layer microchannel patterns. h) 1, 2, and 3, layer microchannel constructs with unpolymerized cell-collagen suspension added. i) 1, 2, and 3, layer microchannel constructs after collagen has been polymerized and F127 rinsed away. Notice that channels in each layer are separate, but share a connection at the edges and center of the construct. Scale bar for images f-i = 10mm. j) Epifluorescent image of bioprinted GFP positive microvascular cells suspended in collagen. In focus channel on left is above the out of focus channel on the right.

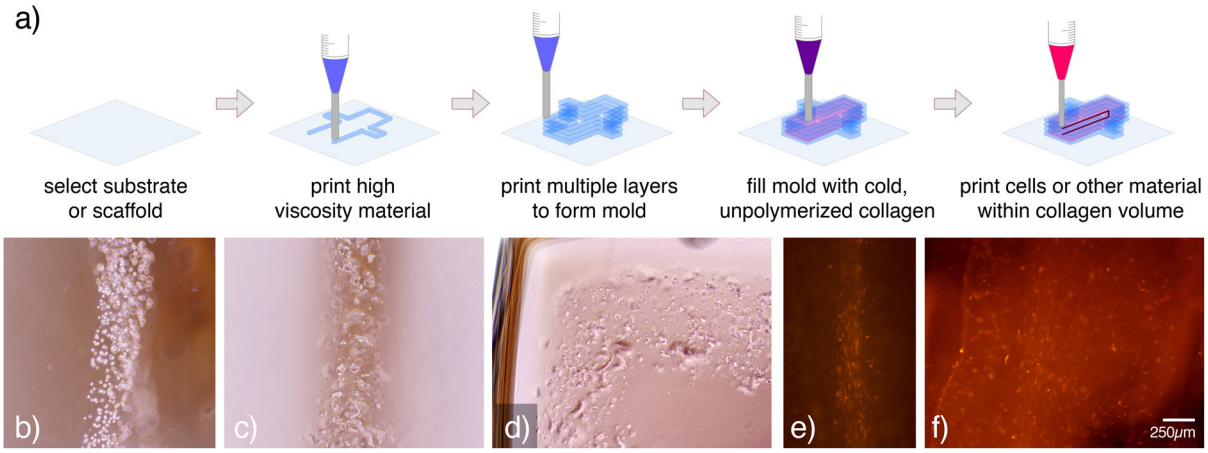

Figure 6.

Example of microvascular cells printed within a cell-free collagen matrix with a 25ga needle. a) Schematic illustrating in-matrix bioprinting. First an F127 mold is printed and then filled with unpolymerized collagen. Next, the bioprinting needle for biological dispensing is lowered into the collagen volume. Biological materials, such as cell-collagen suspensions, are then dispensed into a desired shape within the collagen matrix. b) Individual cell lines were printed within a collagen volume formed into a channel by a surrounding F127 mold. c) Lines of isolated microvessel fragments were also printed within a molded collagen volume. d) Curved lines of microvessel fragments were also printed within collagen matrix. e) After 1 day of in vitro culture, cells begin to form cord-like structures. f) After 5 days of culture, cells migrate throughout the 120μL construct.

Table 1

Comparison of Prominent Bioprinting Methods.

	Ink-Jet Bioprinting	Direct-write Bioprinting
computer designed pattern	yes	yes
method of pattern printing	pattern rasterized into dots	pattern translated into lines
viscosity of printed material	3.5 to 12 mPa*s [21]	30 to > 6×10^7 mPa*s[a]
printed feature height	5 μm [24]	10μm to millimeters [8,70]
printing resolution	1 – 20μm [21,24]	5μm [8]
print multiple materials in single pass	yes [15,21,24]	no [8,70]
nozzle or needle size	20μm to 150μm [15,21,71]	20μm to millimeters [8,30]
dispense cells	yes[15,22,71]	yes [8,27,28]
dispense complex, multi-cellular clusters	no	yes [23,25,29]
cell viability after printing	greater than 85% [22]	up to 98 % [27,30]

[a] viscosities measured with Brookfield Digital Rheometer, model DV-III+

Table 2

Printing Parameters for Pneumatic Dispensing of Hydrogels

F127 Wt%	viscosity (mPa*s)	needle (ga)	pressure (+/− 0.005 PSI)	write height (+/− 0.5 μm)	mean line width (μm)	line width s.e.m.
25	30[a]	20	1	200	1255	32.1
		25	1.5	200	647	9.1
		30	2.5	200	524	25.1
30	1500[a]	20	4	200	993	67.4
		25	14	200	811	20.1
		30	24	200	577	9.4
35	266×10^5[a]	20	9	400	1179	36.2
		25	20	400	938	26.6
		30	50	400	785	15.4
40	$>600 \times 10^6$[a]	20	20	400	898	15.0
		25	45	400	494	8.5
		30	99	300	316	1.4

[a] viscosities measured with Brookfield Digital Rheometer, model DV-III+

Table 3

Printing Parameters for Mechanical Dispensing of Hydrogels

F127 Wt%	viscosity (mPa*s)	needle (ga)	piston linear displacement (+/− 1.5 × 10^{-5} mm/s)	write height (+/− 0.5 μm)	mean line width (μm)	line width s.e.m.
25	30[a]	20	0.005	200	1365	4.9
		25	0.005	200	791	13.9
		30	0.007	200	449	24.3
30	1500[a]	20	0.010	200	917	27.3
		25	0.020	200	842	44.1
		30	0.025	200	492	24.4
35	266 × 10^5[a]	20	0.025	400	954	17.0
		25	0.035	400	726	13.9
		30	0.040	400	597	27.7
40	>600 × 10^6[a]	20	0.025	400	1199	14.8
		25	0.030	400	1125	27.8
		30	0.035	300	339	33.2

[a] viscosities measured with Brookfield Digital Rheometer, model DV-III+